Coulomb-blockade oscillations in a quantum dot strongly coupled to leads

T. Heinzel and A. T. Johnson
Department of Physics, David Rittenhouse Laboratory, 209 South 33rd Street, University of Pennsylvania, Philadelphia, Pennsylvania 19104

D. A. Wharam and J. P. Kotthaus
Sektion Physik der Ludwig-Maximilians Universität München, Geschwister-Scholl-Platz 1, 80539 München, Germany

G. Böhm, W. Klein, G. Tränkle, and G. Weimann
Walter Schottky Institut, Technische Universität München, 85748 Garching, Germany
(Received 22 May 1995)

We report on the behavior of Coulomb-blockade oscillations in a semiconductor quantum dot, when its coupling to the leads is strong, i.e., of the order of the dot's energy-level separation. Under magnetic fields $0.75 \leq B \leq 4$ T, we find a periodic amplitude modulation of both the peaks and the valleys of the conductance resonances. Assuming that only the lowest edge channel carries current, we apply a model, describing partly coherent and partly incoherent electron transport, to explain these modulations. Within this model, the period of the amplitude modulation reflects the filling factor inside the dot. The amplitude of the envelope function is determined by the fraction of electrons scattered inelastically in the dot, the electron temperature, and the transmission of the tunnel barriers that couple the dot to the reservoirs. We show that it is only in the strong coupling regime where we can distinguish between thermal broadening and broadening as a consequence of inelastic scattering. We use this model to estimate the electron temperature as well as the phase-coherence length inside the quantum dot. The modulation of the conductance valleys is related to a periodic modulation of cotunneling rates.

I. INTRODUCTION

State-of-the-art lithography enables two-dimensional electron systems, formed in a GaAs-$Al_xGa_{1-x}As$ heterostructure, to be structured on a submicron length scale. Electrostatically defined small conducting islands (quantum dots) have become subject of a tremendous amount of both experimental and theoretical work.[1] If the coupling Γ of the quantum dot to the nearby electron gas is smaller than the attempt frequency, the number of electrons on the island becomes a well-defined quantity,[2] and single-electron charging effects[3,4] can be observed, provided the charging energy $E_c = e^2/2\mathcal{C}_\Sigma$ necessary to add one single electron to the island is larger than k_BT. Here $\mathcal{C}_\Sigma$ denotes the total capacitance of the island to the environment, and T the electron temperature. One striking effect is the observation of conductance oscillations as a function of an external gate voltage, so-called Coulomb-blockade (CB) oscillations.[5–7] For very low electron occupation numbers of the dot and under strong magnetic fields, elaborate models have been developed to describe the electronic structure,[8] which are in good agreement with experiments.[9] For higher occupation numbers and moderate magnetic fields, usually the constant-interaction picture is used.[10] The quantum dot can be modeled by a circular disk with a parabolic confinement potential, whose eigenspectrum is known as the Darwin-Fock[11] spectrum. Here the energy eigenvalues E_{ml} obey

$$E_{ml} = (2m + |l| + 1)\hbar\sqrt{(\omega_0^2 + \omega_c^2/4)} + \tfrac{1}{2}l\hbar\omega_c \ , \qquad (1)$$

where l is the angular momentum quantum number, m the radial quantum number, ω_c the cyclotron frequency, and ω_0 characterizes the confining potential of the quantum dot.

The width of the dot eigenstates is determined by the coupling of the dot to the leads and by the inelastic scattering rate inside the dot. For a quantum dot in the diffusive regime, it has been shown that electron-electron interactions are the dominant broadening mechanism.[12] For a ballistic quantum dot in the low-coupling regime, the width of the energy states can be obtained by fitting the CB oscillation resonances with a thermally broadened Lorentzian.[13] Since the temperature is low, the only inelastic (i.e., phase destroying) process is electron-electron scattering.

In this paper, we report on amplitude modulations and large-scale envelopes of CB oscillations in the regime of strong coupling of the dot to the leads (i.e., the transmission T of the tunneling barriers is $0.1 \leq T < 1$) and under magnetic fields of $1\ \text{T} \leq B \leq 4$ T. The occupation number is typically 100, although widely tuned (± 70). Periodic modulations of CB oscillations were observed by Staring *et al.*[14] who performed a model calculation, assuming different coupling constants of dot states belonging to different Landau levels (LL's), which qualitatively explained their data. In the present work, we develop a method that models the amplitude modulations quantitatively. Our model is based upon a formalism developed by Büttiker,[15] and explicitly includes the electron temperature, inelastic scattering inside the dot, and, via the indi-

0163-1829/95/52(23)/16638(8)/$06.00 ©1995 The American Physical Society

vidual tunnel barrier transmissions, the coupling Γ of the dot to the leads. We show in a model calculation how these contributions broaden the amplitude modulations. We measured Γ and show that, in the regime of strong coupling, we can distinguish between thermal broadening and broadening by inelastic scattering. Within our model, the electron temperature and the fraction of incoherent transport can thus be extracted from a fit of the *amplitudes* of the CB oscillations.

The outline of the paper is as follows: In Sec. II, we discuss the experimental setup. In Sec. III, the experimental data are presented. In Sec. IV, the model is introduced and applied to our measurements; the range of validity of this approach is discussed. In Sec. V, we focus attention on an interpretation of the valley conductance modulation. We conclude with a summary in Sec. VI.

II. EXPERIMENTAL DETAILS

The measurements were performed in a modulation-doped GaAs-$Al_{0.32}Ga_{0.68}As$ heterostructure with an electron sheet density of 3.6×10^{15} m^{-2} and a mobility of 120 m^2/Vs at $T=4.2$ K, which corresponds to an elastic mean free path of 11.3 μm. A surface gate structure (100-nm Au on 10-nm NiCr) was made using electron-beam lithography. A quantum dot of radius 200 nm was defined by application of negative voltages to the Finger gate F, gates Q_1, Q_2, and C (left inset in Fig. 1). The gate geometry enabeled us to sweep the electrochemical potential of the quantum dot by varying the voltage applied to the center gate V_C. In contrast to most samples, this structure was not inspected with an electron microscope after fabrication, in order to avoid possible radiation damage. Instead, a dummy sample was processed in parallel for control purposes. The sample was inserted in a ^{3}He-^{4}He dilution refrigerator with a base temperature of 25 mK. We have studied the transport properties of the structure in a two-terminal configuration by applying a low-frequency bias voltage (31 Hz, 4.3 μV) and measuring the current with a standard op-amp current-to-voltage conversion circuit. The current resolution in this configuration was 200 fA. A magnetic field up to 14 T could be applied perpendicular to the plane of the two-dimensional electron gas.

Each electrical connection to the sample was fed through a separate ratio-frequency/high-frequency filter. A damping of at least -75 dB in the frequency range between 1 MHz and 3 GHz was measured for these filters.

III. EXPERIMENTAL OBSERVATIONS

If the conductance of the two quantum point contacts (QPC's), formed by gates F, Q_1, and Q_2, drops below $2e^2/h$ (or e^2/h, when spin splitting is resolved), all the electrons on the island are localized, and their number N_e becomes well defined. A sweep of V_C, the voltage applied to the center gate C, changes N_e and leads to periodic CB oscillations.

Figure 1 shows CB oscillations as observed in our structure at various magnetic fields. They set in as soon as the area underneath the center gate is depleted, i.e.,

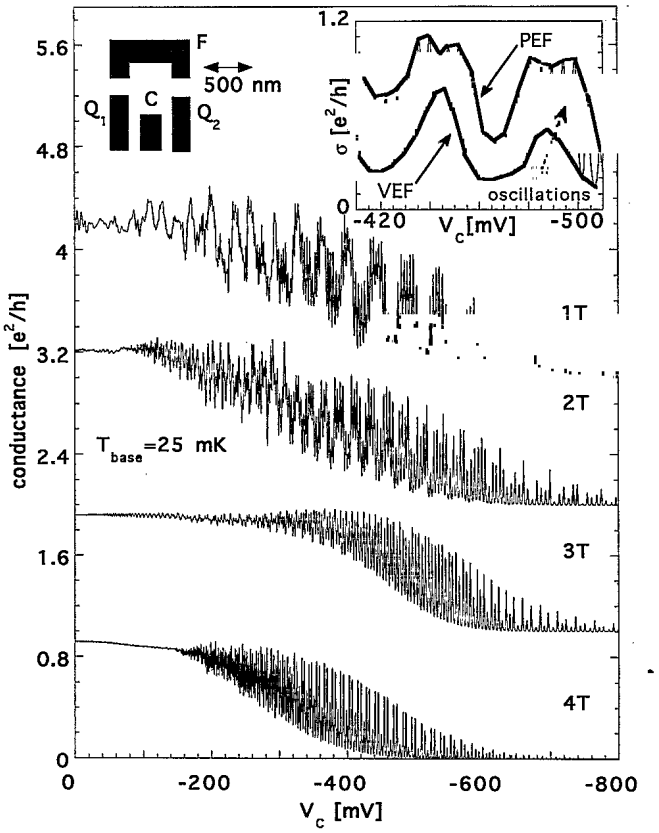

FIG. 1. Measured Coulomb blockade oscillations as a function of the center gate voltage V_C under various magnetic fields. The curves are offset by e^2/h. Left inset: gate structure for the quantum dot. The gates are labeled F, Q_1, Q_2, and C. Right inset: a section of the measurement under $B=1$ T. The CB oscillations show a modulation of the peak envelope function PEF as well as a modulation of the conductance valleys (valley envelope function VEF).

around $V_C\simeq-200$ mV. A rich variety of different amplitude modulations and envelopes is observed. The right inset in Fig. 1 shows a section of the measurement at $B=1$ T. The CB oscillations have a period of about 5 mV in this range of V_C. Their peak conductance shows a quasiperiodic envelope with a higher period (ten CB oscillations per modulation period on average in this case). In the present paper, we focus on a quantitative explanation of this peak envelope function. Moreover, we qualitatively explain the valley envelope function, which is in phase with the peak envelope function. Both envelope-function amplitudes can exceed the amplitudes of the CB oscillations themselves. Although the peak envelope-function amplitudes are very high over the whole range of V_C, the valley envelope function, very pronounced in the regime of high overall conductance, is strongly suppressed at lower center gate voltages. Furthermore, the valley envelope-function amplitude decreases with increasing magnetic field, in contrast to the peak modulation. Both envelope functions follow a smooth large-scale envelope in addition.

Although the change of the energy of the conduction-

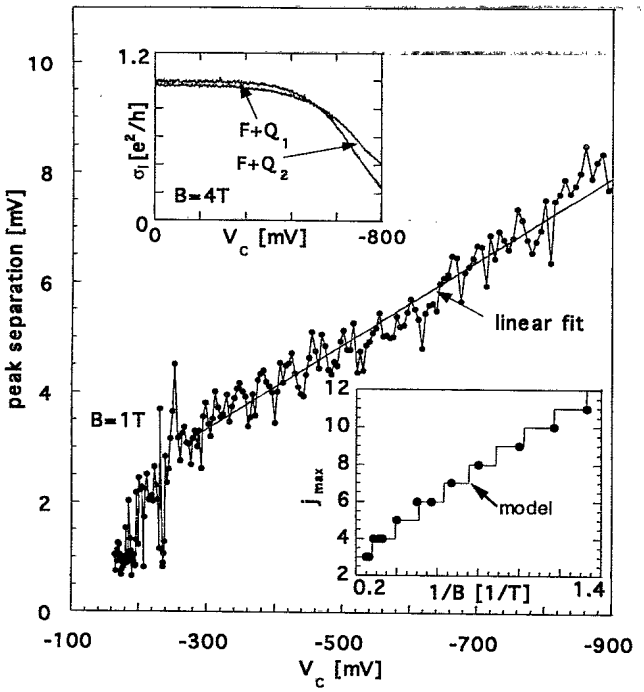

FIG. 2. The peak separation of the CB oscillations as a function of V_C. The linear fits for $\Delta V_C(V_C)$ are almost independent of the magnetic field. Lower inset: The number j_{max} of CB oscillations per modulation period for different magnetic fields. The measurement points are obtained by averaging over all the modulations observed at a particular magnetic field. The model curve is a fit by using Eq. (9). Upper inset: a typical measurement of the influence of the center gate voltage on the transmission of the individual QPC's, formed by gates F and Q_1 and by F and Q_2, respectively.

band bottom inside the dot is the dominant effect of a variation of V_C the individual transmissions of QPC's 1 and 2 are also influenced, due to the stray field of V_C at the site of these tunnel barriers. This dependence can be measured by adjusting one QPC to its working point while keeping the Q gate not used grounded, and measuring its transmission as a function of V_C. We denote these functions by $T_i(V_C)$, $i=1$ and 2 (upper inset in Fig. 2). These functions resemble a Fermi distribution function, as expected for a saddle-point potential barrier in strong magnetic fields.[16] $T_i(V_C)$ varies smoothly for all magnetic fields. The measurements presented in Fig. 1 hence correspond to a study of the behavior of CB oscillations under a smooth transition from high to low coupling of the dot to the leads.

IV. DESCRIPTION OF THE MODEL AND ITS APPLICATION

In this section, we develop a quantitative description for the *peak* envelope function. Following the interpretation of Ref. 14, we assume that only states belonging to the first LL couple to the reservoirs and that the change of the occupation number of higher LLs has to occur via excitation of LL 1 states. This LL-index dependent coupling of the dot states to the leads is, within our model, the origin of the amplitude modulations. Note that this assumption has a pronounced effect on the density of states. Only the states associated with LL 1 are broadened by the nonzero transmission of the tunneling barriers. States belonging to higher LL's have a much sharper density of states, and broaden exclusively as a consequence of inelastic scattering.

For sufficiently high magnetic fields, the LL 1 states of the energy spectrum [Eq. (1)] can be thought of as circulating edge states (i.e., one-dimensional states). We consider the variations in transport through these dot states as their energies are tuned by a sweep in V_C.

The LL 1 states inside the dot can be described as circulating edge states as soon as the cyclotron diameter becomes smaller than the dot radius, that is, when $2\omega_0<\omega_c$.[17] For our sample, this condition is fulfilled for $B\geq 0.65$ T. In this approximation, the energy separation of adjacent LL 1 states inside the dot can be written as[17]

$$\Delta E_{\mathrm{LL1}}=\hbar\frac{\omega_0^2}{\omega_c} . \tag{2}$$

Within a coherent resonant-tunneling model, we determine the phase difference of adjacent circulating edge states of LL 1 from the phase-matching condition $\Delta\Phi=2\pi$, where $\Delta\Phi$, the phase difference electrons accumulate during one round trip inside the dot at different energies, is given by

$$\Delta\Phi=\frac{2\pi\omega_c}{\hbar\omega_0^2}\Delta E . \tag{3}$$

We now quantitatively describe the peak envelope function by calculating the transmission of LL 1 states inside the dot as a function of V_C, B, the electron temperature T, and the fraction β of electrons that suffer an inelastic scattering event inside the dot. This model is based on the work of Büttiker, who developed a formalism for calculating transmission probabilities of one-dimensional (1D) systems coupled to reservoirs via tunnel barriers.[15] Since we are only considering the circulating edge states of LL 1, this model is appropriate for our case. We use T as well as β as fitting parameters. Büttiker models inelastic scattering as a phase-coherence-destroying reservoir between the two tunnel barriers. In our sample, we expect that electron-electron scattering is the only relevant phase-breaking mechanism.

In detail, we assume that the total transmission coefficient of the quantum dot can be written as the sum of a coherent and an incoherent part, i.e.,

$$T(V_C)=T_{\mathrm{coh}}(V_C)+T_{\mathrm{inc}}(V_C) . \tag{4}$$

At zero temperature and without inelastic scattering inside the dot, the coherent part is given by an Airy for-

mula,[18] similar to the description of the transmission of optical resonators.[19] In the same way as finite coupling to the leads does, inelastic scattering events homogeneously broadens the LL 1 states and thus influence the coherent transmission. To take into account the finite electron temperature, we integrate over the thermally smeared Fermi function $f(E)$. In this general case, the coherent part is given by[15]

$$T_{\mathrm{coh}}(V_C)=\int\left[(1-\beta)T_1(V_C)T_2(V_C)\left[-\frac{df(E)}{dE}\right]\Big/Z(V_C,E)\right]dE\ , \tag{5}$$

with

$$Z(V_C,E)=1+(1-\beta)^2[1-T_1(V_C)][1-T_2(V_C)]+2(1-\beta)\sqrt{[1-T_1(V_C)][1-T_2(V_C)]}\cos(\Phi(V_C,E))$$

and

$$\Phi(V_C,E)=\frac{2\pi\omega_c}{\hbar\omega_0^2}[E-E_d(V_C)-\tfrac{1}{2}\hbar\omega_c]\ . \tag{6}$$

The LL 1 states are described by the phase the electrons accumulate inside the dot, $\Phi(V_C,E)$ [Eq. (6)], broadened by the nonzero transmission of the tunnel barriers, and by inelastic scattering events. Furthermore, $E_d(V_C)$ is the energy of the conduction-band bottom inside the quantum dot at the position of the maxima of the CB oscillation resonances. The determination of this function from the experimental data is described below.

For fully incoherent transport at $T=0$, T_{inc} is given by the product of the probability for the electron to enter the dot, which is equal to the backscattering probability S_b, times the fraction of scattered electrons emerging from the scatterer in the forward direction.[15] If we denote the forward-scattering probability by S_f, this fraction can be written as $S_f/(S_b+S_f)$. Here we assume that the electrons suffer only a single scattering event while inside the dot. Since we expect the electron-electron-scattering length to be large compared to the dot size, this assumption is well justified. Including a finite temperature leads to the incoherent part

$$T_{\mathrm{inc}}(V_C)=\left\{\int S_b(V_C,E)\left[-\frac{df(E)}{dE}\right]dE\right\}\left\{\int S_f(V_C,E)\left[-\frac{df(E)}{dE}\right]dE\right\}\Big/\left\{\int[S_b(V_C,E)+S_f(V_C,E)]\left[-\frac{df(E)}{dE}\right]dE\right\} \tag{7}$$

with

$$S_{b,f}(V_C,E)=\beta T_{1,2}(V_C)\{1+(1-\beta)[1-T_{2,1}(V_C)]\}/Z(V_C,E)\ . \tag{8}$$

Equation (8) is derived in detail in Ref. 15, and represents the sum over all possible paths that lead to backscattering or forward scattering, respectively.

Note that β and $T_i(V_C)$ enter symmetrically in $Z(E,V_C)$ as well as in $S_{b,f}(E,V_C)$. These contributions to the broadening of the LL 1 states are thus indistinguishable. Hence, in order to extract β, it is essential to measure $T_i(V_C)$.

The QPC transmissions $T_i(V_C)$ are, in principle, also dependent upon E. Experimentally, however, we are only able to measure the coefficients $T_i(V_C)$ and $T(V_C)$. Since the energy scale over which the transmission of the QPC's varies, given by the 1D subband separation within the QPC's, is much larger than k_BT for the temperatures present in our studies, we neglect the influence of a finite temperature on $T_i(V_C)$. Hence we use $T_i(V_C)$ in our calculations, the experimentally determined functions. The thermal smearing of the Fermi function cannot, however, be neglected inside the quantum dot. Here the mean energy-level separation is comparable to k_BT, which makes thermal excitations significant.

In the following paragraph, we focus on the effects of temperature and inelastic scattering on the peak envelope functions. For completely coherent transport at zero temperature, we expect sharp peak envelope-function resonances with a peak value of 1, as shown in Fig. 3(a), broadened only by the nonzero transmission of the tunneling barriers. For this model calculation, we have assumed $T_i(V_C)$ to be Fermi functions, as shown in the inset of Fig. 3(a). Both finite temperature [Fig. 3(b)] and inelastic scattering [i.e., $\beta>0$, Fig. 3(c)] reduce the amplitude of the peak envelope function. However, at high coupling, a finite temperature only smears out the peak envelope-function resonances. In contrast, inelastic scattering also reduces the average transmission. The physical interpretation of this effect is straightforward:

for the coherent fraction of the electron transport, the average transmission T_a of the structure is given just by the transmission of one of the two tunneling barriers. The incoherent fraction, however, sees the two barriers in series, which leads to a reduction of T_a. Roughly, T_a can be estimated by $T_a \sim T_i[(1-\beta)+\beta/2]$. For completely incoherent transport, the oscillation in the peak envelope function vanishes, and T_a is half the transmission of a single barrier [Fig. 3(c)]. This distinct difference at high coupling enables us to distinguish between thermal broadening and broadening as a consequence of inelastic-scattering events.[20] Furthermore, according to Eq. (2), we expect a reduction of the amplitude of the peak envelope-function oscillations for increasing magnetic fields.

Experimentally, we find a significantly broadened peak envelope-function amplitude (Fig. 1). The peak transmission decreases smoothly approximately one order of magnitude when V_C is reduced from -200 to -800 mV.

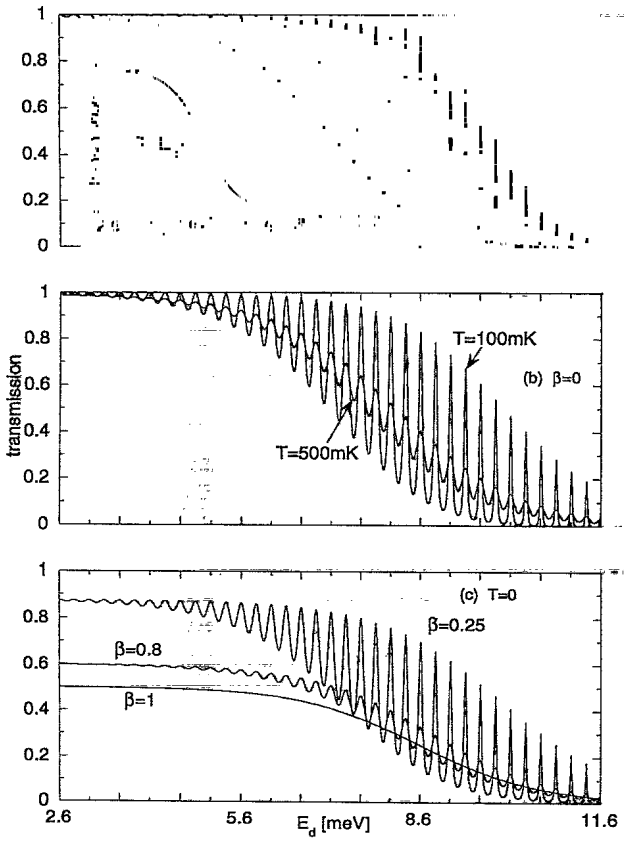

FIG. 3. Calculated peak envelope function. A Fermi energy of 11.6 meV and a confining potential characterized by $\omega_0=1.2\times10^{12}$ s^{-1} has been assumed. (a) Completely coherent transmission at $T=0$, inset: the assumed transmission of the QPC's as a function of the dot energy. (b) Effect of a finite temperature. (c) Effect of inelastic scattering at $T=0$. Note the distinct difference between (b) and (c), namely the reduction of the average transmission at high QPC conductances in (c) compared to (b).

The peak envelope function can be modeled by fitting T and β to the measurements. A separate analysis of the temperature dependence of the linewidth of the CB oscillation resonances[13] (not shown) implies that the electron temperature is roughly 100 mK.

To link the model to the experimental data, we extract the dot Fermi energy E_F and the confinement potential strength ω_0 from fitting the observed number of CB oscillations per modulation period to the magnetic-field dependence of the number of occupied LL's, $j_{\max}$. For a parabolic confinement potential, $j_{\max}$ is given by

$$j_{\max}=\mathrm{INT}\left[\frac{2}{\hbar\omega_c}\left[\frac{E_F+0.5\hbar\omega_c}{1+\omega_0^2/\omega_c^2}\right]\right]. \tag{9}$$

in Eq. (9), INT denotes rounding to the nearest integer value. The fit shown in the lower inset of Fig. 2 yields $E_F=7.81$ meV and $\omega_0=7.08\times10^{11}$ s^{-1}. The spin is taken into account by the factor of 2. Each value for $j_{\max}$ in Fig. 2 is an average over all peak envelope-function modulations in a center gate voltage sweep at a fixed magnetic field. We do not find a systematic dependence of $j_{\max}$ on V_C, indicating that the filling factor inside the dot remains unchanged. Magnetoconductance oscillations in this regime[21] show a period of $\Delta B=36$ mT, corresponding to a dot radius of $r_d\approx200$ nm, in very good agreement with a calculation of r_d using our fit values for E_F and ω_0.

Furthermore, we have to determine $E_d(V_C)$. The peak positions of the CB oscillations provide points $E_{d,i}$ at $V_{C,i}$, where i is the index of a CB peak. For our calculations, we make $E_d(V_C)$ continuous between these points of relevance by interpolating between the CB oscillation peaks and integrating $dE_d(V_C)=(\Delta E_d/\Delta V_C(V_C))dV_C$ over V_C. Here ΔE_d denotes the energy shift of the conduction-band bottom under a change of the dot's occupation number by 1, and is obtained from our dot model [Eq. (2)], $\Delta E_d=\hbar\omega_0^2/j_{\max}\omega_c$. The corresponding center gate voltage difference ΔV_C (the CB oscillation peak separation) is, to a good approximation, a linear function of V_C (Fig. 2). This linear dependence of ΔV_C on V_C reflects the change of the capacitance between the center gate and the dot when V_C is varied.

Gate voltage characteristics of a single quantum point contact (i.e., simultaneous sweeps of gate F and one of the Q gates with the second Q gate and gate C grounded) show spin splitting in the lowest one-dimensional subband for $B>2$ T (not shown). We thus assume that below 2 T, the two spin states of LL 1 couple equally from the reservoirs to the dot, and for higher magnetic fields only LL 1 states with spin-up have a nonzero coupling. The QPC's were adjusted to equal conductances (upper inset in Fig. 2), since asymmetries between $T_1(V_C)$ and $T_2(V_C)$ reduce the amplitude of the resonances in the peak envelope function [Eqs. (5) and (6)]. After rescaling the QPC transmission functions to an energy scale by the method described above, we use them in Eqs. (5)–(8). Figure 4 shows fits for different magnetic fields. Results of our fits are summarized in Table I. From our calculations, we estimate an effective electron tempera-

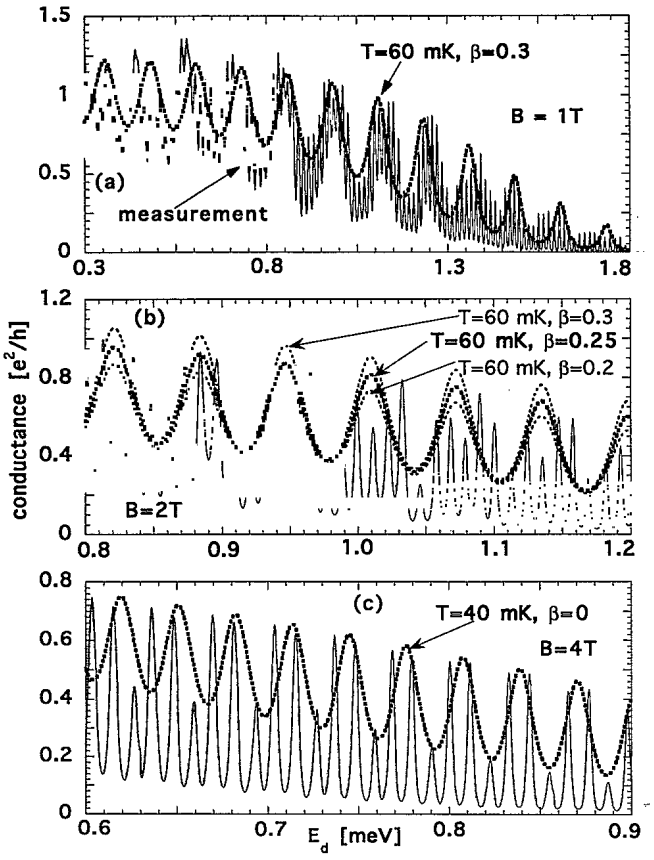

FIG. 4. Fits of the measured peak envelope function at $B=1$ T (a), 2 T (b), and 4 T (c). The CB oscillations have been rescaled to an energy scale as described in the text. In (b), we show the fits used to estimate the uncertainty of the inelastic fraction.

ture of $T=(60\pm30)$ mK. The uncertainty is comparable to that we obtain from an analysis of the temperature dependence of the line shape of individual CB oscillation resonances. The parameter β decreases significantly with increasing magnetic field. This indicates that the phase-coherence length inside the quantum dot increases rapidly when B is increased. The fact that the oscillation amplitude of the peak envelope function does not decrease under increasing B, as expected from Eq. (2), can thus be traced back to the increased coherence of the transport. Further measurements are necessary to determine this dependence in greater detail. An increased I_Φ with increasing B has also been found by Liu *et al.*[22] by analyzing the Fourier amplitudes of Aharanov-Bohm-type oscillations in mesoscopic rings in the case of CB being absent. Note that our model assumes that the phase is completely randomized in a single electron-electron-scattering event, as measured in the ballistic regime.[23] We can find the inelastic-scattering length I_Φ from the expression $(1-\beta)=\exp(-2\pi r_d/I_\Phi)$ (see Table I).

TABLE I. Summary of the parameters as obtained from the fits of the peak envelope function and the estimated phase coherence length I_Φ.

Magnetic field (T)	Electron temperature (mK)	β	I_Φ (μm)
1	60±30	0.3±0.05	3.5
2	60±25	0.25±0.05	4.35
3	50±20	<0.05	>24.4
4	40±10	<0.05	>24.4

To bring the calculated peak envelope functions in phase with the measurements, we shifted the calculated transmission in energy by small amounts. We attribute the necessity of such a shift due the influence of the voltage applied to Q_2 on the transmission of QPC_1, and vice versa. This shift is, however, not experimentally accessible without the quantum dot being formed. Since these gates are much farther separated from each other than the Q gates from the center gate, we believe this to be a small effect.

We would like to point out that the model developed here is for intermediate magnetic fields and not too small occupation numbers. At higher magnetic fields, the quantum dot develops an additional internal structure.[24,25] Due to the modulation of the screening properties of the electron gas, compressible regions are formed, separated by incompressible stripes. The condition for this internal structure to occur is that the magnetic length is larger than the width of these incompressible stripes.[24] Most strikingly, frequent magnetoconductance oscillations are observed[25] for $\nu<2$ a regime where the constant-interaction picture predicts very infrequent energy-level crossings as a function of the magnetic field. At low magnetic fields, on the other hand, the model of circulating edge states is no longer justified. As B goes to zero, the characteristic splitting of the states with high Γ approaches $\hbar\omega_0$. Indeed, for small magnetic fields, we find huge, reproducible amplitude modulations that dominate over the CB oscillations for high Γ (Fig. 5).

Strong electron-electron interactions at low dot occupation numbers provide another limiting factor. In this case, the assumption of a single-particle spectrum is no

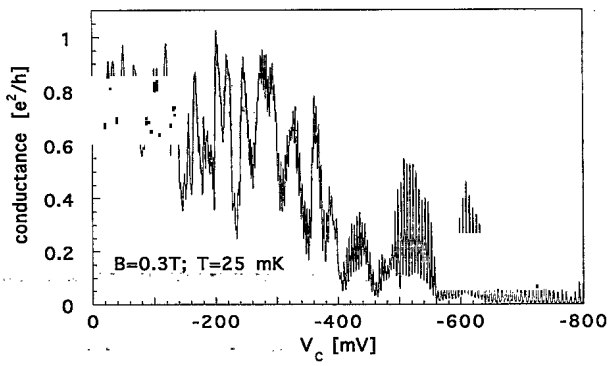

FIG. 5. CB oscillations in a weak magnetic field. Nonperiodic, reproducible conductance fluctuations with huge amplitude are observed. The CB oscillations are modulated and dominate the measurement for $V_C \leq -400$ mV.

longer justified, although recently it has been shown that even in an interacting system composed of only 2 or 3 electrons, there exist quasiselection rules that provide a preferential coupling of center-of-mass modes to the leads.[26] It would thus be very interesting to investigate the behavior of CB oscillation amplitude modulations in extremely small quantum dots.

V. MODULATION OF THE CONDUCTANCE VALLEYS

The observed valley envelope function (Fig. 1) is in phase with the peak envelope function, indicating a similar physical origin. It is, however, much more strongly suppressed than the peak envelope function at both high magnetic fields and low coupling [Fig. 6(a)]. Since CB is established, we interpret the valley modulation as a consequence of cotunneling currents.[27] Inelastic cotunneling generates an excitation in the dot, and the transport is incoherent. A periodic valley envelope function due to inelastic cotunneling can only occur when two LL 1 states take part in the transport. Their energy separation is, however, large compared to both the temperature as well as the bias voltage. We conclude that elastic cotunneling is the origin of the modulation of the conductance valleys, and is of the same order of magnitude as inelastic cotunneling in our experiments. For a quantitative description, the finite temperature is significant. We thus restrict ourselves to a qualitative interpretation. To illustrate our explanation, we consider the case of a filling factor of 2 [Figs. 6(b) and 6(c)]. If we assume, as above, that only states belonging to LL 1 couple to the leads, elastic cotunneling also occurs preferentially via these states. If the peak envelope function is maximum, a LL 1 state is in resonance with the Fermi energy in the leads, and hence we can expect a correspondingly high cotunneling current in the conductance valley nearby, i.e., a maximum in the valley envelope function [Fig. 6(b)]. If the peak envelope function, however, is in a minimum, the energy between E_F in the reservoirs and the closest LL 1 state is maximized, which leads to a reduction in the cotunneling current as well [Fig. 6(c)]. Since the cotunneling currents[27] scale with Γ^2, these valley modulations are much stronger suppressed than the peak modulation (which scales with Γ) when the coupling is reduced. The decrease of the oscillation amplitude of the valley envelope function under increasing magnetic field is expected from Eq. (2). The energy separation of LL 1 states decreases under increasing magnetic field, and virtual excitations in these states are less suppressed.

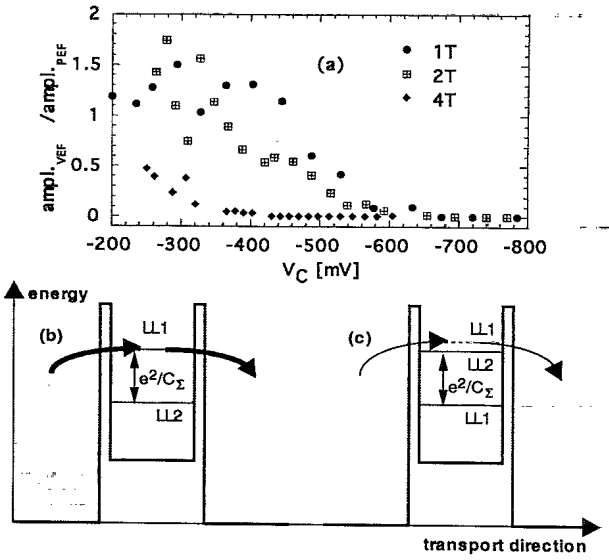

FIG. 6. (a) The ratio of the oscillation amplitude of the valley envelope function to that of the peak envelope function for different magnetic fields. The valley modulations are much more strongly suppressed than the peak modulations under decreasing coupling as well as under increasing magnetic field, indicating the virtual character of the valley current. (b) and (c) Suggested origin of the valley envelope function oscillations: if the lowest empty state inside the dot is a LL 1 state, we expect, as a consequence of its high coupling to the leads, a high rate of elastic cotunneling (b). If the lowest unoccupied state belongs to a higher LL, cotunneling currents arise from excitation into a LL 1 state nearby (c) and are thus strongly reduced.

VI. SUMMARY

We investigated CB oscillations in a strongly coupled quantum dot in magnetic fields from 1 to 4 T. We found amplitude modulations of both the CB oscillation peaks and valleys. We have developed a quantitative model for the peak envelope function, based upon previous theoretical work of Büttiker. We used this method to determine the electron temperature and the fraction of electrons that are scattered inelastically while traversing the dot, giving an estimated phase-coherence length. We found strong evidence for an increased phase-coherence length as the magnetic field increases. Modulation of the conductance valleys has its origin in a partly phase coherent cotunneling current.

ACKNOWLEDGMENTS

We have enjoyed fruitful discussions with C. Kane, S. Ulloa, F. Hofmann, and A. Govorov. Financial support by the University of Pennsylvania and the Deutsche Forschungsgemeinschaft is gratefully acknowledged.

[1]For a review, see *The Physics of Few-Electron Nanostructures,* edited by L. J. Geerligs, C. J. P. M. Harmans, and L. P. Kouwenhoven (North-Holland, Amsterdam, 1993).

[2]D. J. Thouless, Phys. Rev. Lett. **39**, 1167 (1977).

[3]*Single Charge Tunneling,* edited by H. Grabert, J. M. Martinis, and M. H. Devoret (Plenum, New York, 1991).

[4]Special issue on single charge tunneling, Z. Phys. B **85**, 3 (1991).

[5]J. H. F. Scott-Thomas, S. B. Field, M. A. Kastner, H. I. Smith, and D. A. Antoniadis, Phys. Rev. Lett. **62**, 583 (1989).

[6]U. Meirav, M. A. Kastner, and S. J. Wind, Phys. Rev. Lett. **65**, 771 (1990).

[7]L. P. Kouwenhoven, A. T. Johnson, N. C. van der Vaart, C. J. P. M. Harmans, and C. T. Foxon, Phys. Rev. Lett. **67**, 1626 (1991).

[8]P. Hawrylak, Phys. Rev. Lett. **71**, 3347 (1993); S.-R. Yang, A. H. MacDonald, and M. D. Johnson, *ibid.* **71**, 3194 (1993); J. J. Palacios, L. Martin-Moreno, G. Chiappe, E. Louis, and C. Tejedor, Phys. Rev. B **50**, 5760 (1994); D. Pfannkuche, V. Gudmundsson, and P. A. Maksym, *ibid.* **47**, 2244 (1993).

[9]R. C. Ashoori, H. L. Störmer, J. S. Weiner, L. N. Pfeiffer, K. W. Baldwin, and K. W. West, Phys. Rev. Lett. **71**, 613 (1993).

[10]C. W. J. Beenakker, Phys. Rev. B **44**, 1646 (1991).

[11]C. G. Darwin, Proc. Cambridge Philos. Soc. **27**, 86 (1931); V. Fock, Z. Phys. **47**, 446 (1928).

[12]U. Sivan, F. P. Milliken, K. Milkove, R. Rishton, Y. Lee, J. M. Hong, V. Boegli, D. Kern, and M. DeFranza, Europhys. Lett. **25**, 605 (1994); U. Sivan, Y. Imry, and A. G. Aronov, *ibid.* **28**, 115 (1994).

[13]E. B. Foxman, P. L. McEuen, U. Meirav, N. S. Wingreen, Y. Meir, P. A. Belk, N. R. Belk, M. A. Kastner, and S. J. Wind, Phys. Rev. B **47**, 10 020 (1993).

[14]A. A. M. Staring, B. W. Alphenaar, H. van Houten, L. W. Molenkamp, O. J. A. Buyk, M. A. A. Mabesoone, and C. T. Foxon, Phys. Rev. B **46**, 12 869 (1992).

[15]M. Büttiker, Phys. Rev. B **35**, 4123 (1987); IBM J. Res. Dev. **32**, 63 (1988).

[16]H. A. Fertig and B. I. Halperin, Phys. Rev. B **36**, 7969 (1987).

[17]After a transformation of Eq. (1) to the quantum numbers $k=2m+|l|+1$ and $j=m+0.5(l+|l|)+1$ (j is the spin-degenerate LL index and k the zero-field harmonic-oscillator quantum number), we define $\Delta E_k = F \quad F$. and find for $2\omega_0/\omega_c < 1$ the approximation ΔE_k ' a value independent of j and k. Using $k=1$ gives Eq. (2). Note that the error of this approximation is of the order $(\omega_0/\omega_c)^4$, and vanishes rapidly as soon as $2\omega_0$ becomes smaller than ω_c.

[18]A. T. Johnson, L. P. Kouwenhoven, W. de Jong, N. C. van der Vaart, C. J. P. M. Harmans, and C. T. Foxon, Phys. Rev. Lett. **69**, 1592 (1992).

[19]See, for example, A. Yariv, *Quantum Electronics* (Wiley, New York, 1975).

[20]The two broadening mechanisms also lead to different line shapes; inelastic scattering and finite coupling give a Lorentzian profile, while finite temperature gives a Gaussian line shape. However, this difference cannot be seen in our data.

[21]T. Heinzel, D. A. Wharam, J. P. Kotthaus, G. Böhm, W. Klein, G. Tränkle, and G. Weimann, Phys. Rev. B **50**, 15 113 (1994).

[22]J. Liu, W. X. Gao, K. Ismail, K. Y. Lee, J. M. Hong, and S. Washburn, Phys. Rev. B **50**, 17 383 (1994).

[23]A. Yacobi, U. Sivan, C. P. Umbach, and J. M. Jong, Phys. Rev. Lett. **66**, 1938 (1991).

[24]P. L. McEuen, E. B. Foxman, J. Kinaret, U. Meirav, M. A. Kastner, N. S. Wingreen, and S. J. Wind, Phys. Rev. B **45**, 11 419 (1992); I. K. Marmorkos and C. W. J. Beenakker, *ibid.* **46**, 15 562 (1992); D. B. Chklovskii, B. I. Shklovskii, and L. I. Glazman, *ibid.* **48**, 11 120 (1993).

[25]P. L. McEuen, E. B. Foxman, U. Meirav, M. A. Kastner, Y. Meir, N. S. Wingreen, and S. J. Wind, Phys. Rev. Lett. **66**, 1926 (1991).

[26]D. Pfannkuche and S. E. Ulloa, Phys. Rev. Lett. **74**, 1194 (1995).

[27]D. V. Averin and Y. V. Nazarov, Phys. Rev. Lett. **65**, 2446 (1990).